Macromolecules

pubs.acs.org/Macromolecules Article

Alternating Gyroid Stabilized by Surfactant-like Triblock Terpolymers in IS/SO/ISO Ternary Blends

Pengyu Chen, Frank S. Bates, and Kevin D. Dorfman*

Cite This: *Macromolecules* 2023, 56, 2568−2577 Read Online

ACCESS | Metrics & More | Article Recommendations | Supporting Information

ABSTRACT: Block polymers self-assembled into chiral alternating-gyroid (G^A) morphologies are desirable templates for fabricating photonic materials. Recent self-consistent field theory (SCFT) calculations on a model system predicted that adding a minuscule amount of ABC triblocks into a blend of thermodynamically symmetric double-gyroid-forming AB and BC diblocks with immiscible A and C blocks stabilizes G^A. Here, we use SCFT to investigate the feasibility of this method in practice by computing the phase behaviors of ternary mixtures of poly(isoprene-*b*-styrene) (IS), poly(styrene-*b*-ethylene oxide) (SO), and poly(isoprene-*b*-styrene-*b*-ethylene oxide) (ISO). Addition of ISO indeed stabilizes G^A; however, the phase window is relatively narrow, due to the packing frustration induced by the mismatch in preferred domain sizes between IS and SO diblock copolymers. Designing the system to have comparable diblock domain sizes significantly enhances the relative stability of G^A against the competing alternating lamellae, and this stability is also sensitive to the degree of polymerization of the ISO midblock. Moreover, the stabilization of alternating morphologies is sensitive to temperature, and less ISO is needed at lower temperatures. The effect of some other design parameters, such as diblock volume fraction, is also investigated. These computational results provide insights into possible experimental strategies for producing G^A and highlight the sensitivity of network phase formation to asymmetries in the thermodynamic parameters.

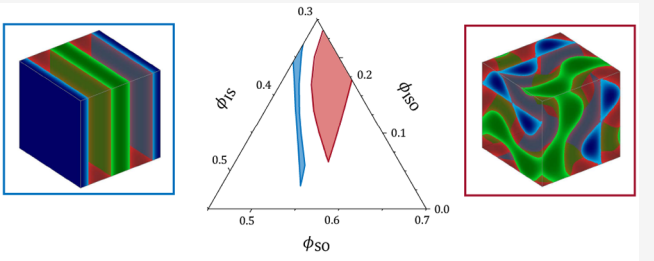

INTRODUCTION

Co-continuous network morphologies self-assembled by block copolymers have extraordinary potential for applications in photonics,[1,2] membrane separations,[3] and energy conversion.[4] The most commonly observed network morphology is the double gyroid (DG), a tricontinuous phase comprising two interpenetrating 3-fold connected networks of the same chemistry embedded within a matrix of a distinct chemical constitution.[5] In AB diblock copolymers, the DG phase can be conceptualized as resulting from localizing the chain ends of the majority B blocks on the Schoen gyroid (G) minimal surface.[6,7] A related bicontinuous morphology, single gyroid (SG), arising instead from situating the junctions between A and B blocks along the G surface, has two interpenetrating gyroid networks of different chemistry. The inherited chirality of SG grants it extraordinary optical properties, which gives rise to the structural color of butterfly wings and bird species,[8−10] and also makes it a potential structure for fabricating photonic materials with complete photonic band gaps according to calculations.[11] However, SG has not been experimentally observed in block copolymer self-assembly, and the only prediction of its stabilization is in a linear pentablock copolymer melt.[12]

Alternating gyroid (G^A), which has been observed experimentally and predicted theoretically in linear ABC triblock terpolymer melts, offers alternative approaches to produce complete band gap materials.[13−16] In contrast to DG, the two interpenetrating A and C networks of G^A are of distinct chemistry, as illustrated in Figure 1, and thus introduce the desired chirality. Based on the computational work by Lequieu et al.,[2] sophisticated design of bottlebrush ABC triblock terpolymers with a large refractive index contrast between the A and C monomers that form the opposing networks should produce photonic band gaps. Moreover, solvent extraction after selectively etching one of the two networks of G^A and backfilling with a metal can produce SG-structured materials with unusual photonic properties.[17,18]

Despite the great potential of G^A in photonic applications, there are still limitations in making G^A through self-assembly of ABC triblock terpolymer polymers. Most importantly, the relatively small stability window of G^A in the enormous parameter space of an ABC triblock system makes it difficult to target the desired experimental conditions.[15,16] In ABC triblock terpolymer melts, phase behavior in the mean-field

Received: December 9, 2022
Revised: February 22, 2023
Published: March 7, 2023

https://doi.org/10.1021/acs.macromol.2c02485
Macromolecules 2023, 56, 2568−2577

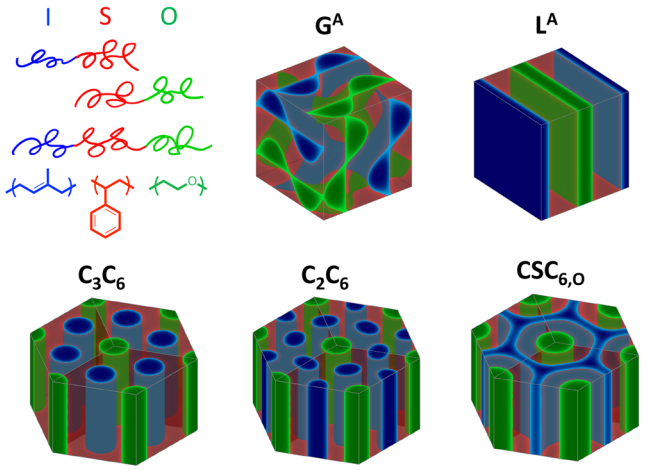

Figure 1. Illustration of the ternary blend system with poly(styrene-*b*-isoprene) (IS) diblock polymers, poly(styrene-*b*-ethylene oxide) (SO) diblock polymers, and poly(isoprene-*b*-styrene-*b*-ethylene oxide) (ISO) triblock polymers. Composition profiles of selected candidate phases obtained from self-consistent field theory (SCFT) calculations. Blue, red, and green colors indicate regions where the local concentrations of I, S, and O monomers are greater than 0.5, respectively.

limit is governed by five parameters if the differences between statistical segment lengths b are neglected: independent volume fractions f_A and f_B and the segregation strengths $\chi_{AB}N$, $\chi_{BC}N$, and $\chi_{AC}N$, where χ is the Flory–Huggins interaction parameter and N is the degree of polymerization of the polymer chain. Precise control over the total molecular weight, block polymer composition, and temperature is required to stabilize G^A, which makes this strategy less promising when considering large-scale production. In a recent study by Park et al.,[19] an alternative strategy for producing G^A was proposed based on block polymer blends. They investigated the free energies of binary mixtures of DG-forming AB and BC diblock copolymers using self-consistent field theory (SCFT), and the metastable G^A was predicted to be nearly degenerate with the stable macrophase-separated DG states. This marginal metastability suggests that solvent casting can potentially trap the binary diblock mixtures in a metastable G^A state. Moreover, adding a minuscule amount of ABC triblock terpolymer was predicted to open up the stability window of G^A through surfactant-like action, which connects the opposing A and C networks and destabilizes macrophase separation between the two DG states.[19] This blending method avoids the need for precise control over polymer compositions and offers the possibility of selectively removing one network by extraction using a selective solvent or through polymer degradation, attractive approaches for creating SG-structured materials.[20]

Although the calculations by Park et al.[19] suggest a promising route to access G^A, there are still limitations in the system they studied. Owing to the enormous parameter space for the AB/BC/ABC ternary system, a thermodynamically symmetric model of block polymers was adopted for simplification. In their model, they assumed equal statistical segment lengths b_A, b_B, and b_C, equal Flory–Huggins interaction parameters χ_{AB} and χ_{BC}, and equal diblock volume fractions $f_{A(AB)}$ and $f_{C(BC)}$, where the subscript in parentheses indicates the relevant block polymers. Such an idealized model is convenient for theoretical study, but it is unrealistic, as such symmetric parameters are impossible to realize in practice and may have a significant influence on the formation of the G^A phase. An idealized G^A has two sets of gyroid struts of equal size such that the B matrix is largely uniform in thickness and centered along the G minimal surface, which minimizes its free energy. Any asymmetry induced by the differences in statistical segment lengths, Flory–Huggins interaction parameters, or diblock volume fractions will cause G^A to deviate from this ideal configuration and hinder its formation. For example, in a nonfrustrated ABC neat melt, the introduction of molecular asymmetry distorts the phase diagram and causes a narrower phase window of G^A.[16] The formation of the G^A phase in AB/BC/ABC ternary blends is also likely to be sensitive to the molecular asymmetry. Therefore, additional investigation of a more realistic polymer system with asymmetric parameters is required to verify the feasibility of the blending method.

Here, we utilize SCFT to study the phase behavior of the ternary mixture of poly(isoprene-*b*-styrene) (IS), poly(styrene-*b*-ethylene oxide) (SO), and poly(isoprene-*b*-styrene-*b*-ethylene oxide) (ISO) under different temperatures. The effects of some other polymer parameters, such as diblock volume fractions, are also investigated. The IS/SO/ISO ternary blend was selected as a practical route toward G^A for the following reasons. First, the phase behavior of ISO triblock terpolymer melts has been well studied both theoretically and experimentally, and the stability window of G^A has been predicted and experimentally identified.[15,16,21,22] Second, the IS/SO/ISO mixture is a nonfrustrated system, meaning that the interaction parameter between end blocks of the ABC triblock terpolymers is much larger than that between either end block and the middle block, i.e., $\chi_{AC} \gg \chi_{AB} \sim \chi_{BC}$.[23] In such a system the self-assembled morphologies tend to avoid A/C contacts, which is a prerequisite for the stabilization of G^A. While we focus here on the IS/SO/ISO system, we note that other AB/BC/ABC ternary systems with nonfrustrated triblock terpolymers such as polyisoprene-*b*-polystyrene-*b*-poly(2-vinylpyridine) (ISP)[13,14] and poly(1,2-butadiene)-*b*-polystyrene-*b*-poly(methyl methacrylate) (BSM)[24] are also promising candidates, and we anticipate the insights gained here will be relevant if one were to pursue ISP-based or BSM-based systems to produce G^A.

METHODS

Self-Consistent Field Theory. SCFT is the most powerful tool for studying the phase behavior of block polymers. In particular, its ability to accurately predict stability regions of ordered morphologies at a low computational cost has been widely validated by experimental phase maps of different block polymer systems.[25−27] To study the phase behavior of the IS/SO/ISO ternary system, both canonical and grand canonical ensemble SCFT are applied. The detailed implementation of SCFT and the procedure to construct phase diagrams using grand canonical SCFT calculations can be found in the paper by Park and co-workers.[19]

Our SCFT calculations are performed using the open-source software package Polymer Self-Consistent Field software (PSCF) developed by Morse and co-workers.[28] In the pseduo-spectral method, which PSCF uses to solve the modified diffusion equations (MDEs), periodic solutions of MDEs are discretized by a computational contour step Δs and grid points in real space.[27,29] The contour step size is chosen as $\Delta s = 0.01N_{IS}$ for the input files for our calculations, where N_{IS} is the degree of polymerization of the IS diblock copolymers. When the input step size is not commensurate with an even discretization of the contour of a given block, PSCF selects a smaller Δs that is as close as possible to the input value while also discretizing the chain into equal segments. A tolerance of 10^{-5} for

https://doi.org/10.1021/acs.macromol.2c02485
Macromolecules 2023, 56, 2568−2577

the convergence was used based on the definition in ref 27. The grid sizes used for the free energy calculations of all candidate phases are 36^n, where n is equal to 1, 2, or 3 depending on the dimension of the periodic structures.

To initialize our SCFT calculations, the following alternating phases are considered as candidate structures: alternating gyroid (G^A), alternating lamellae (L^A), alternating diamond (D^A), squared-packed alternating cylinders (C_4^A), hexagonally packed alternating cylinders with I minority cylinders on 3-fold rotation axes and O majority cylinders on 6-fold rotation axes (C_3C_6), and hexagonally packed alternating cylinders with I minority cylinders on 2-fold rotation axes (C_2C_6). The inverted morphologies with majority I cylinders C_6C_3 and C_6C_2 are also included. An alternating O^{70} phase was considered, but the SCFT calculations fail to converge in the parameter space of interest. Four core−shell morphologies are taken into consideration: core−shell hexagonally packed O cylinders ($CSC_{6,O}$), core−shell hexagonally packed I cylinders ($CSC_{6,I}$), perforated core−shell double gyroid with O networks (CSG_O), and perforated core−shell double gyroid with I networks (CSG_I). Monomer density profiles of selected morphologies are provided in Figure 1. For the IS or SO diblock-rich regions, we consider lamellae (L), hexagonally packed cylinders (C_6), double gyroid (DG), and the body-centered cubic sphere-packing phase (BCC). A complete list of the candidate phases can be found in Figures S1 and S2 of the Supporting Information.

Physical Models for IS/SO/ISO Ternary Blends. The major differences between the idealized model in the work by Park et al.[19] and our more realistic model of IS/SO/ISO ternary blends are the unbalanced interaction parameters between χ_{IS} and χ_{SO}, as well as the conformational asymmetry introduced by the differences in the statistical segment lengths b_i between polymer chains of different chemical identities. The choice of statistical segment lengths is relatively straightforward. We use b_I = 6.0 Å, b_S = 5.5 Å, and b_O = 7.8 Å for a monomer reference volume of 118 Å^3, which are adapted from published results.[30] We do not consider the effect of temperature on the statistical segment lengths, as the most important effect of temperature lies in the segregation strengths. The selection of χ parameters, however, is more complicated owing to the inconsistency between reported values.[1,31,32] Here, we use the interaction parameters from previous work by Tyler et al.:[16]

$$\chi_{IS} = \frac{19.2}{T} - 0.0078 \quad (1)$$

$$\chi_{SO} = \frac{29.8}{T} - 0.0229 \quad (2)$$

$$\chi_{IO} = \frac{90.0}{T} - 0.0579 \quad (3)$$

where T is the absolute temperature. The same model was applied to investigate the phase behavior of linear ISO triblock polymer melts using SCFT, and the results were largely consistent with the experimental observations.[15,16]

Since the parameter space of the IS/SO/ISO blends is prohibitively large and the phase behavior is expected to be complicated, it is not practical to explore the impact of all the physical parameters. Hence, the ternary phase diagram of the mixture is first studied with all the parameters constant except for the blend composition. We start from a temperature of T = 100 °C, which is the lowest allowed experimental temperature for the polymers to be in a rubbery state.[15] Unless otherwise noted, the total chain lengths of the diblock polymers are fixed at $N_{IS} = N_{SO} \equiv N = 300$, and therefore the χN values for the diblock polymers are $\chi_{IS}N$ = 13.1 and $\chi_{SO}N$ = 17.1. Using the same degree of polymerization N as the diblock copolymers, the segregation strength between I and O is $\chi_{IO}N$ = 55.0. The volume fractions of I and O monomers in the diblock polymers are chosen as $f_{I(IS)}$ = 0.41 and $f_{O(SO)}$ = 0.425, where the subscript in parentheses indicates the relevant block polymer, such that DG is the stable morphology for both IS and SO diblock polymer melts at this temperature. Although multiplying $f_{O(SO)}$ by N_{SO} results in a noninteger $N_{O(SO)}$, this is not a problem in the SCFT calculations because the polymer chain is discretized by the predetermined contour step size Δs that discretizes the chain into equal segments. The design for the third component, the ISO triblock terpolymer, is less restricted. It has been demonstrated that, in the idealized AB/BC/ABC blend system, the exact composition of the ABC triblock polymer is not critical for the stabilization of G^A provided that the B block is sufficiently long to bridge the A and C gyroid networks;[19] we will explore this extrapolation of this conclusion for the symmetric system to the IS/SO/ISO system. Hence, for most of our calculations, we simply use the same relative degree of polymerization and volume fractions used in the previous study on the idealized system, which results in an L^A-forming triblock terpolymer with a total degree of polymerization N_{ISO} = 403 and end blocks with the same length $N_{I(ISO)} = N_{O(ISO)}$ = 128.5. To investigate the effect of temperature, we simply update the χ-parameters at increased temperatures using eqs 1−3 while keeping the other physical parameters unchanged. The χ- and χN-values for different temperatures are provided in Table 1.

Table 1. List of χ-Parameters and χN Values for N = 300 at Different Temperatures

T (°C)	$\chi_{IS}/\chi_{IS}N$	$\chi_{SO}/\chi_{SO}N$	$\chi_{IO}/\chi_{IO}N$
100	0.0437/13.2	0.0570/17.1	0.1833/55.0
125	0.0404/12.1	0.0519/15.6	0.1681/50.4
150	0.0376/11.3	0.0475/14.3	0.1548/46.4

RESULTS

As was the case in prior work,[19] we begin first by examining the phase behavior of the diblock blend. Figure 2 provides the relative free energy of the IS/SO binary blend system for different candidate phases at 100 °C as a function of the concentration of SO diblock copolymers, ϕ_{SO}. Unlike the single-component block polymer systems, in which only microphase separation can occur, macrophase separation is also possible in blended systems.[33−35] Therefore, the free energy is plotted with respect to the common-tangent line between the free energy curves of DG-forming IS and DG-forming SO diblocks for easier visualization, and the original free energy plot without subtracting the common-tangent line is provided in Figure S3.

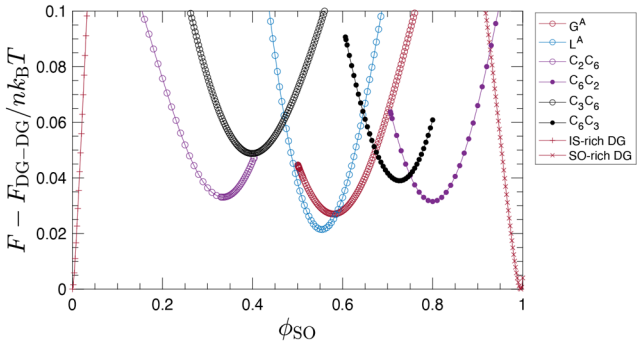

Figure 2. Free energy differences for different phases relative to the common-tangent line between diblock-rich DG phases in the IS/SO binary mixture as a function of SO diblock polymer compositions ϕ_{SO} at T = 100 °C.

Figure 2 shows that mixing DG-forming IS and SO diblocks leads to macrophase separation into two diblock-rich DG phases, qualitatively similar to previous work.[19] Surprisingly, in contrast to what was observed for the idealized AB/BC system in previous work,[19] G^A does not outcompete all the other

https://doi.org/10.1021/acs.macromol.2c02485
Macromolecules 2023, 56, 2568−2577

metastable phases for an IS/SO blend. Instead, L^A has a lower free energy minimum than G^A. Moreover, the lowest free energy of G^A relative to macrophase separation is 0.027 nk_BT, which is much larger than the 0.001 nk_BT difference predicted in the idealized system.[19] Such a large free energy gap, along with the competing L^A phase, should make it difficult to trap this diblock mixture in the metastable G^A phase through solvent casting. While our primary focus is on the G^A phase, we note that at the cylinder-forming compositions, C_2C_6 and C_6C_2, have lower free energy minima than the more commonly observed alternating cylindrical phases C_3C_6 and C_6C_3.[36,37] We will return to the cylinder-phase selection issue, which is subtle, in the Discussion section.

To stabilize the alternating phases against macrophase separation, a small amount of ISO triblock polymers should be added to the system. According to the previous report in an AB/BC/ABC ternary system,[19] such triblock additives act like a surfactant that bridges the opposing A and C domain in the alternating phases and inhibit macrophase separation by raising the free energies of the AB-rich or BC-rich DG phases through the inclusion of the incompatible ABC triblock. To examine how the triblock surfactant impacts the phase behavior in the more realistic chemical system under investigation here, Figure 3(a) provides portions of the phase diagram of the ternary IS/SO/ISO mixture at T = 100 °C. Only the bottom portion of the diagram for $\phi_{ISO} < 0.25$ is computed, as adding more ISO triblock is anticipated to complicate the phase behavior, and the surfactant-like stabilization effect by the triblocks will disappear.

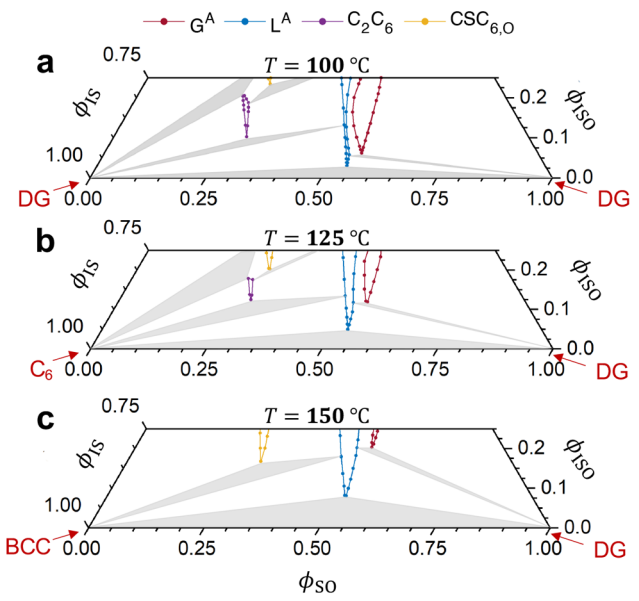

Figure 3. Ternary phase diagrams of the IS/SO/ISO blend system at a temperature of (a) 100 °C, (b) 125 °C, and (c) 150 °C. Dotted lines indicate the phase boundaries for different alternating morphologies. The dots indicate the computed boundary points. Shaded regions are the three-phase-coexistance regions. At the IS-rich and SO-rich corners of the phase diagrams marked by the arrows, there exists very small stability regions of diblock-rich phases. The enlarged portions of these regions are provided in Figure S4.

Compared to the idealized blend system, where only diblock-rich DG, C_3C_6, C_6C_3, and G^A were predicted to be stable, the phase behavior of the IS/SO/ISO mixture is much more complicated. As illustrated in Figure 3(a), G^A is indeed stabilized by adding a small amount of ISO triblock polymer. However, the smallest amount of triblock needed to open up the phase window is $\phi^*_{G^A,ISO} = 0.062$, which is much larger than the value $\phi^*_{G^A,ABC} = 0.001$ in the idealized model.[19] Our SCFT calculations also predict a narrow stability window of L^A, which is not present in the thermodynamically symmetric system. Moreover, near the blend compositions where C_3C_6 was predicted to be the equilibrium morphology in the thermodynamically symmetric system, C_3C_6 is now metastable in the IS/SO/ISO blend. Rather, SCFT predicts stability windows of $CSC_{6,O}$ and a new morphology C_2C_6, which contains hexagonally packed cylinders of the I blocks on 2-fold axes and hexagonally packed cylinders of the O blocks on 6-fold axes (see Figure 1). Finally, mainly due to the discrepancy in statistical segment lengths and χ-parameters between IS and SO diblock polymers, the phase diagram we compute is highly asymmetric. Besides the fact that both G^A and L^A stability windows are located in regions where ϕ_{SO} is higher than ϕ_{IS}, C_6C_2 and $CSC_{6,I}$, the inverted phases of C_2C_6 and $CSC_{6,O}$, are metastable at higher ϕ_{SO}.

Since our purpose here is to facilitate the experimental preparation of G^A materials, it is worth investigating the phase behavior at different temperatures, as temperature changes the interactions between polymers and is well known to be a key factor in phase selection.[38] Although accurately modeling the dependence of χ on temperature to match experiments remains a major challenge,[1,31] especially in systems with more than two monomer types, the predicted change in phase behavior as temperature varies can still provide useful information about the system once an appropriate model of χ is selected. Here, we use the model described in the Methods section and study the phase behavior of the IS/SO/ISO ternary system at T = 100, 125 and 150 °C. As temperature increases, the χ values decrease, and thus the segregation strength χN decreases. As listed in Table 1, increasing the temperature from 100 °C to 125 °C leads to a decrease in $\chi_{IS}N$ from 13.1 to 12.1, and $\chi_{SO}N$ from 17.1 to 15.6. It should be noted that in IS diblock neat melts with the lower $\chi_{IS}N$, C_6 becomes the stable morphology rather than DG Figure 3(b). Further increasing the temperature to 150 °C lowers $\chi_{IS}N$ to 11.3, moving the IS diblock neat melt into the sphere-forming region. Meanwhile, as $\chi_{SO}N$ decreases to 14.3, DG remains the equilibrium morphology in SO diblock polymer melts.

Figure 3(b) and (c) provide the bottom part of the ternary phase diagrams at T = 125 and 150 °C. A stable window of G^A is still predicted at higher temperatures, despite of the fact that the IS diblocks no longer form DG in a neat melt, revealing that stabilization of G^A in a mixture of non-DG-forming diblocks with a small amount of surfactant-like triblock additives is possible. By comparing the phase diagrams at different temperatures, a noticeable shift of $\phi^*_{G^A,ISO}$ to higher compositions at higher temperatures is observed, where $\phi^*_{G^A,ISO}$ is the lowest ISO triblock composition needed to stabilize G^A. Similarly, the critical ISO composition for L^A stabilization, $\phi^*_{L^A,ISO}$, shifts to higher compositions as temperature increases, resulting in a much larger three-phase-coexistance region at the low-ϕ_{ISO} region of the ternary phase diagram at higher temperature.

https://doi.org/10.1021/acs.macromol.2c02485
Macromolecules 2023, 56, 2568−2577

In addition to the fact that more ISO triblock polymers are needed to stabilize any alternating phase at higher temperatures, temperature also alters the relative stabilities of competing alternating phases. As temperature increases, the stability window of G^A gets narrower, and, contrarily, the phase window of L^A becomes wider. Additionally, the phase window of C_2C_6 gets smaller at 125 °C and eventually vanishes at 150 °C, which leads to a widened stability window of $CSC_{6,O}$.

DISCUSSION

Domain Size Matching between Diblock Copolymers.

The selection of alternating morphologies in ternary blends is determined by the competing effects of macrophase and microphase separation, as well as the competition between metastable binary phases formed by two types of diblock copolymers. For the case of G^A in AB/BC blends, prior work established that the addition of a small amount of ABC triblock destabilizes the macrophase separated state and leads to the emergence of the alternating phase.[19] Although the phase behavior of the IS/SO/ISO ternary system appears to be complicated, the differences in phase behaviors between the thermodynamically symmetric AB/BC/ABC system[19] and the system we study here can mostly be explained by the mismatch in preferred domain sizes between the diblocks, which primarily affects the competition between different alternating phases rather than the competition between an alternating phase and macrophase separation. In the thermodynamically symmetric case, AB and BC diblock polymers self-assemble into DG phases of the exact same size, and thus in the mixture they tend to form A and C domains of equal size near the symmetric composition $\phi_{AB} = \phi_{BC} = 0.5$. In the more realistic system we study, however, the domain sizes of DG formed by IS and SO diblocks are different. Compared to $\chi_{SO}N = 17.1$, IS has a smaller segregation strength $\chi_{IS}N = 13.1$, which results in a smaller preferred domain size for the IS diblock copolymers. This is evidenced by the domain size ratio $d_{SO} = 1.30d_{IS}$ obtained from unit-cell size calculations of DG-forming IS and SO diblock neat melts. Accordingly, in a compositionally symmetric blend, the I domain is smaller than the O domain. Such a mismatch in preferred domain sizes leads to the formation of different alternating phases in the IS/SO/ISO ternary mixture.

Interfacial area and variation in domain thickness cannot be optimized simultaneously except for the lamellae phases, which causes packing frustration.[39] In an ideal G^A structure with left-handed and right-handed gyroid struts of equal size, the matrix is largely uniform in thickness and is centered on the G minimal surface.[7] As a result, the chain-stretching penalties mainly come from the concave struts, and the enthalpic penalties are minimized as the G minimal surface is an area-minimized surface. In the IS/SO/ISO ternary system, the IS and SO diblock polymers tend to form gyroid struts of different sizes. In this situation, there is no way to form a uniform matrix without severely distorting the domain structure, which will also lead to a significant increase in chain-stretching penalties. This is evidenced by the composite density profile of G^A in an IS/SO binary mixture at symmetric composition in Figure 4, where distorted gyroid struts in the I domain and a nonuniform matrix formed by S monomers are visible. Moreover, for G^A with asymmetric domain sizes, the center of the matrix is shifted away from the G minimal surface, which is not enthalpically favorable due to the increased interfacial area. Both enthalpic and entropic penalties

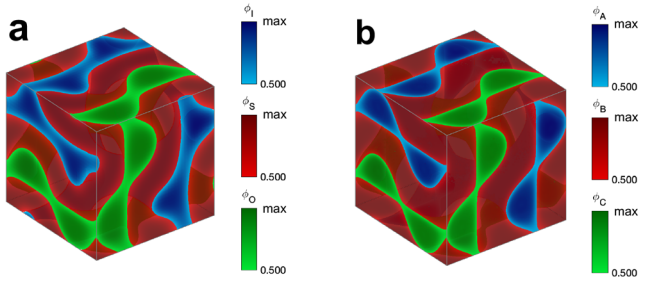

Figure 4. Monomer density profiles of G^A in a compositionally symmetric binary mixture of (a) IS and SO diblock copolymers at T = 100 °C and (b) thermodynamically symmetric AB and BC diblock copolymers. The maxima of monomer densities are $\phi_I^{max} = 0.916$, $\phi_S^{max} = 0.936$, $\phi_O^{max} = 0.990$, and $\phi_A^{max} = \phi_B^{max} = \phi_C^{max} = 0.994$.

in forming G^A are exacerbated by the domain mismatch, and the destabilization of G^A opens up the possibilities for competing phases to occur. While L^A is the only observed competing morphology of G^A in the ternary phase diagrams in Figure 3, the potential for hybrid network phases[40] such as the sphere−diamond and sphere−gyroid phases to become stable with increasing asymmetry of the ternary blend system exists, although this falls outside the scope of our current investigation.

In contrast to the destabilized G^A, the layer structures of L^A accommodate the mismatch in preferred domain sizes much more easily. When building L^A with I and O domains of incommensurate sizes, packing frustration can be minimized by simply adjusting the thicknesses of the uniform layers without deforming the domain interfaces. Correspondingly, L^A has a lower minimal free energy in the binary diblock mixtures compared to G^A, which is what we observed in Figure 2. In addition, the distinct effects of the domain-size mismatch on G^A and L^A explain the stability window of L^A in the predicted phase diagram in Figure 3(a). The fact that ϕ_{SO} for the stability window of L^A is closer to the symmetric compositions also suggests that L^A is less influenced by the domain-size discrepancy.

To further validate our hypothesis regarding the influence of the preferred domain sizes, we investigate the free energy changes of G^A and L^A as we alter the ratios between the preferred domain sizes of IS and SO diblocks. Intuitively, when N_{IS} is increased, the relative stability of G^A compared to L^A is anticipated to increase until a certain point where $d_{IS} = d_{SO}$ is satisfied. Further increasing N_{IS} will lead to a decrease in the relative stability of G^A. The most straightforward way to illustrate this effect is to compute the free energy of G^A and L^A as a function of N_{IS} while keeping the blend composition constant. However, the results of such calculations can be misleading, because changing N_{IS} also changes the I, S, and O monomer fractions in the mixture. To resolve this problem, free energy calculations need to be conducted over a range of blend composition.

Figure 5 illustrates the relative free energy change of different phases as a function of blend composition in the binary IS/SO mixture at different N_{IS}. Figure 5(a) is the same free energy plot shown in Figure 2, with all the cylindrical phases removed for easier visualization. Here, d_{IS} is smaller than d_{SO} at $N_{IS} = 300$. The domain size mismatch leads to a large free energy gap between G^A and L^A and also causes a notable shift in the composition corresponding to the free energy minimum. Figure 5(b) shows a similar plot for N_{IS} =

https://doi.org/10.1021/acs.macromol.2c02485
Macromolecules 2023, 56, 2568−2577

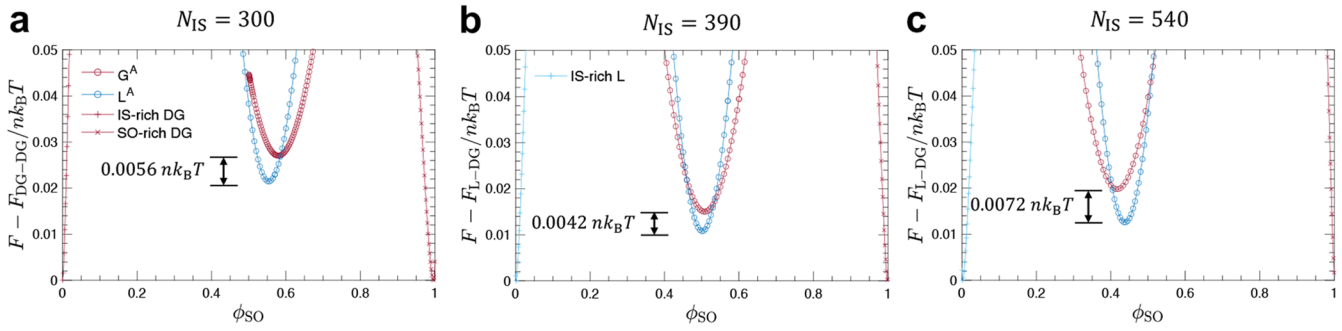

Figure 5. Free energy differences between different phases and the common-tangent line between diblock-rich phases in the IS/SO binary mixture as a function of ϕ_{SO} at T = 100 °C, with a degree of polymerization of IS diblock polymer N_{IS} equal to (a) 300, (b) 390, and (c) 540.

390. Increasing χN_{IS} causes a phase change of the neat IS diblock from DG to L. With this increased chain length, SCFT predicts that d_{IS} of the metastable DG is the same as d_{SO} of the stable DG. By matching the preferred domain sizes, an enhancement in the relative stability of G^A is observed; the energy gap between G^A and L^A narrows from 0.0056 nk_BT to 0.0042 nk_BT. Further increasing to N_{IS} = 540 in Figure 5(c) regenerates the mismatch between domain sizes, which results now in a larger energy gap between G^A and L^A, as well as a noticeable shift of the free energy minimum of G^A to lower ϕ_{SO}. Similar calculations performed with the IS/SO/ISO ternary blends at a fixed ϕ_{ISO} are provided in Figure S5, and the results are consistent with the trend we observe here in the binary mixture, albeit harder to interpret in the ternary mixture. All of these results suggest that resolving the domain-size matching problem increases the relative stability of G^A, despite the fact that the increased $\chi_{IS}N$ moves the neat IS diblock melt into the L-forming region.

The domain size mismatch problem also explains the absence of the alternating hexagonally packed cylinder phase C_3C_6. In contrast to the thermodynamically symmetric case, C_3C_6 is not predicted to be a stable phase in the IS/SO/ISO ternary mixture. Analysis of the monomer density profile in Figure 6(a) shows that the C_3C_6 phase is severely distorted throughout the state space of interest. Instead of forming circular cylinders, the cylinders in the I-rich domains of C_3C_6 tend to have triangular shapes, reflecting the large degrees of packing frustration. This phenomenon can be explained again by the incommensurate domain sizes between the I and O domains. In an idealized case with only IS and SO cylindrical micelles of equal size, these micelles can self-assemble into a hexagonally close-packed structure with two I-rich cylinders, one O-rich cylinder, and a matrix of S that has nearly uniform thickness in each unit cell. If the IS micelles shrink, even though the IS and SO micelles can still touch after shrinking the unit cell, there will be some unfilled space between the IS cylindrical micelles if we were to treat the micelles as rigid. Since these cylindrical micelles formed by block copolymers are not rigid and must fill space, S polymer chains in the diblocks have to stretch in order to fill the void in the nonuniform matrix to avoid severe deformation of the cylinders. The triangular shape of I-rich cylinders C_3C_6 reduces the distances between I/S interfaces along the line that connects the two I-cylinders, and thus S polymer chains from IS diblocks can fill the space between the I-cylinders with less stretching, as illustrated by the monomer density profile of IS diblocks in Figure 6(d). However, such a reshape also increases the chain-stretching penalties in the I-rich cylinders.

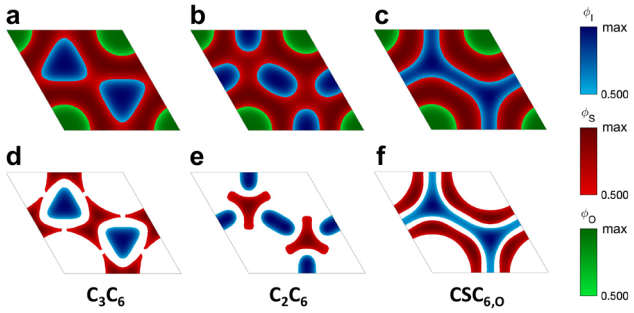

Figure 6. Monomer density profiles of (a) C_3C_6, (b) C_2C_6, and (c) $CSC_{6,O}$ from SCFT solutions. The maxima of local monomer densities in different candidate structures are (a) $\phi^{max}_{C_3C_6,I}$ = 0.937, $\phi^{max}_{C_3C_6,O}$ = 0.995, (b) $\phi^{max}_{C_2C_6,I}$ = 0.931, $\phi^{max}_{C_2C_6,S}$ = 0.919, $\phi^{max}_{C_2C_6,O}$ = 0.995, (c) $\phi^{max}_{CSC_{6,O},I}$ = 0.880, $\phi^{max}_{CSC_{6,O},S}$ = 0.921, and $\phi^{max}_{CSC_{6,O},O}$ = 0.995. Monomer density distribution of IS diblock polymers of (d) C_3C_6, (e) C_2C_6, and (f) $CSC_{6,O}$. The maxima of local monomer density for I and S monomers in IS diblock polymers are (d) $\phi^{max}_{C_3C_6,I(IS)}$ = 0.689, $\phi^{max}_{C_3C_6,S(IS)}$ = 0.605, (e) $\phi^{max}_{C_2C_6,I(IS)}$ = 0.721, $\phi^{max}_{C_2C_6,S(IS)}$ = 0.799, (f) $\phi^{max}_{CSC_{6,O},I(IS)}$ = 0.673, and $\phi^{max}_{CSC_{6,O},I(IS)}$ = 0.583. The monomer distributions of ISO triblock polymers, as well as the junction density distribution, are provided in Figures S6 and S7, respectively.

Therefore, C_3C_6 turns out to be a metastable morphology in the thermodynamically asymmetric IS/SO/ISO blend system. The metastability of C_6C_3 can be explained using a similar analysis.

The destabilization of C_3C_6 opens up the possibility for another morphology to become the equilibrium phase. Instead of forming a highly frustrated C_3C_6, a stability window of C_2C_6 is observed in the cylinder-forming region of the ternary phase diagram. As illustrated in Figure 6(b), the main differences between C_2C_6 and C_3C_6 are the arrangements of the I-cylinders. In this new arrangement, the space between the I-cylinders can be filled by IS diblock copolymers from three nearby cylinders instead of two in C_3C_6, as illustrated in Figure 6(e). Moreover, the I-cylinders are not forced to reshape in a way that causes a dramatic increase in chain-stretching penalties due to the increased number ratio of I- to O-cylinders. As a result, C_2C_6 has a lower degree of packing frustration and thus outcompetes C_3C_6. In the high-ϕ_{SO} region of the ternary diagram, however, neither C_6C_3 nor C_6C_2 is predicted to be stable. Canonical calculations in Figure S8 show that these phases have much higher free energies

https://doi.org/10.1021/acs.macromol.2c02485
Macromolecules 2023, 56, 2568−2577

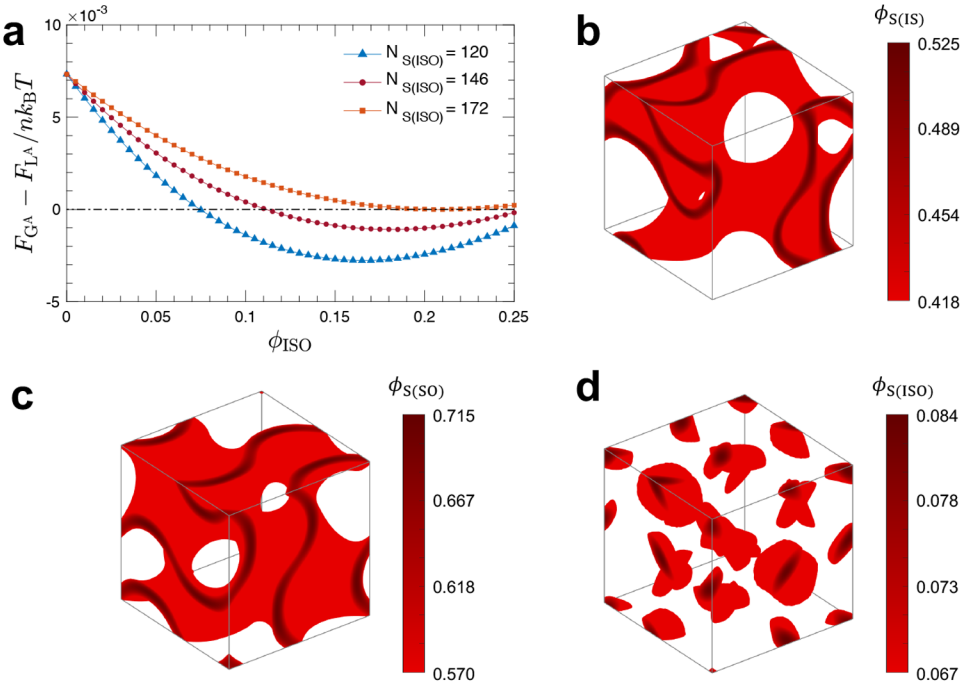

Figure 7. (a) Relative free energies of G^A compared to L^A as a function of ϕ_{ISO} with different $N_{S(ISO)}$ at a fixed ϕ_I/ϕ_O monomer ratio of 0.70 at T = 100 °C. S monomer density profiles of (b) IS diblock, (c) SO diblock, and (d) ISO triblock terpolymers in G^A with $N_{S(ISO)}$ = 146. The cutoff values are set to be 80% of the maximum local S monomer density for each type of polymers.

compared to the common-tangent lines between SO-rich DG and G^A. Their metastability can also be justified by the domain-size mismatch argument. For both C_6C_3 and C_6C_2, there is one I cylinder and multiple O cylinders in one unit cell. The fact that the preferred domain size of the O domain is larger makes it even harder to fill up the space evenly with polymer chains without introducing high degrees of packing frustrations.

Given the complexity of a ternary blend system with three types of monomers, there are indeed numerous structure candidates that may outcompete C_2C_6 and be stable at different composition in the cylinder-forming region. Another alternating cylindrical phase that has similar free energy is $CSC_{6,O}$, the core−shell cylindrical phase with O-cylinders. Figure 6(c) shows that the I domain of $CSC_{6,O}$ shares some common features with both C_3C_6 and C_2C_6. The 3-fold "connector" in the I-shell of $CSC_{6,O}$ resembles the triangle-like I-cylinders of C_3C_6, while the flatter interface of the "tube" is similar to the elliptical I-cylinders of C_2C_6. The fact that $CSC_{6,O}$ is only stable at high ϕ_{ISO} makes it less interesting, because the phase behavior at higher ϕ_{ISO} can potentially be complicated by other unconsidered phases and macrophase separation accompanied by an ISO-rich phase. Some other exotic cylinder phases that have been predicted or experimentally observed, such as the sphere−cylinder hybrid phases, may also be stable in this system.[40−42] We considered two of such phases, with "aligned" and "misaligned" I-spheres arranged in the hexagonally packed O-cylinders,[40] and neither of them converges to a stable structure in our SCFT calculations. Although a thorough investigation of all the possible phases can potentially provide interesting results, it is out of the scope of this work.

Selective Space Filling of ISO Triblock Terpolymers. So far, we have discussed the competition between different candidate phases largely based on the domain-size matching problem between diblock polymers, while the effects of the triblock as a bridging component between the opposing domains have not yet been explored. As shown in the ternary phase diagrams in Figure 3, it is clear that the ISO triblock additive suppresses macrophase separation and stabilizes alternating phases by connecting the I and O domains. The effect of ISO triblock polymers on the relative stability of competing alternating phases is less obvious.

To elucidate the effects of ISO triblock terpolymers, we perform SCFT calculations in the canonical ensemble at a fixed ϕ_I/ϕ_O value of 0.70 at T = 100 °C, and the free energy differences between G^A and L^A as a function of ϕ_{ISO} with $N_{S(ISO)}$ = 146 are provided in Figure 7(a). Since the same triblock terpolymers are used to compute the ternary phase diagram in Figure 3(a), the line along which the canonical calculations are performed can be marked on the phase diagram (Figure S9). According to Figure 7(a), adding ISO triblock polymers lowers the relative free energies of G^A compared to L^A before ϕ_{ISO} reaches 0.185, and addition of more ISO destabilizes G^A. The enhancement in the stability of G^A by increasing the amount of ISO additives is the result of selective space-filling behavior of the ISO triblocks in the formation of G^A. Since G^A is a complex three-dimensional network phase, there exists an optimal orientation and location for ISO triblocks so that they alleviate the packing frustration within the nonuniform domains. As illustrated in Figure 7(b)−(d), the S monomers of ISO triblocks concentrate in certain regions of the matrix, while the S monomers in the diblocks distribute in a more uniform manner throughout the matrix. Unlike in G^A, the one-dimensional L^A phase does not possess the degree of freedom for ISO triblocks to fill the space differently. Therefore, the introduction of ISO triblocks increases the relative stability of G^A compared to L^A for ϕ_{ISO} < 0.185. Adding more ISO triblock polymers is of less interest, because when ϕ_{ISO} becomes substantial, it is anticipated to lose

https://doi.org/10.1021/acs.macromol.2c02485
Macromolecules 2023, 56, 2568−2577

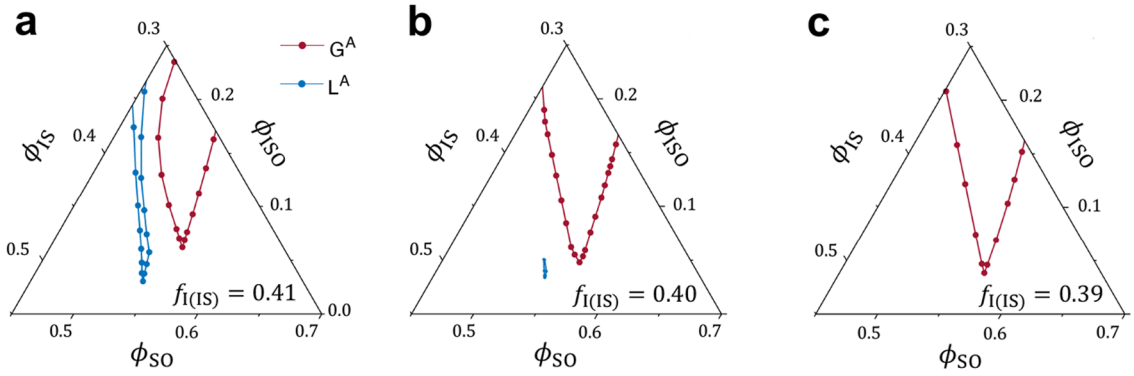

Figure 8. Portions of the IS/SO/ISO ternary phase diagrams at T = 100 °C with a block volume fraction of IS diblock $f_{I(IS)}$ equal to (a) 0.41, (b) 0.40, and (c) 0.39.

its surfactant-like action. Since the ISO triblock polymers in our system are predicted to form L^A in a neat melt, it is unsurprising that the relative stability of L^A increases when more ISO triblock polymers are introduced into the system.

Similar analyses are presented in Figure 7(a) for ISO triblock terpolymers with different midblock lengths while keeping the lengths of end blocks constant, i.e., $N_{I(ISO)}$ = $N_{O(ISO)}$ = 128.5. Although previous calculations by Park et al.[19] suggest that the surfactant-like effect of the ABC triblock additives on stabilizing G^A over macrophase-separated states is insensitive to the exact composition of the triblock terpolymers, our results here show that the exact ISO triblock compositions matter in the competition between G^A and L^A phases. According to Figure 7(a), the stabilization effect from the selective space filling of ISO triblock terpolymers is preserved for ISO triblock terpolymers with different midblock lengths, as indicated by the decrease in relative free energy of G^A as ϕ_{ISO} increases when ϕ_{ISO} is small for different types of triblock additives. However, the extents of stabilization differ for different ISO triblock terpolymers. ISO triblock terpolymers with a shorter midblock have a stronger stabilization effect, as evidenced by the lower relative free energy of G^A for $N_{S(ISO)}$ = 120. For ISO triblock terpolymers with longer midblock, the selective-space-filling effect is weakened because excess S monomers have to locate in nonoptimal regions and thus cannot relieve packing frustration (Figure S10). As a result, G^A fails to outcompete L^A when triblock terpolymers with a longer midblock ($N_{S(ISO)}$ = 172) are added to the blend system, as illustrated in Figure 7(a). These results suggest the importance of the triblock composition in the experimental design of a similar blend system for producing G^A, especially when undesired competing morphologies such as L^A are observed.

Effects of Temperature. According to the computed phase diagrams in Figure 3, the IS-rich and SO-rich phases tend to macrophase separate at higher temperatures, and therefore more ISO triblock polymers are needed to stabilize alternating phases. The overall increase in ϕ^*_{ISO} for the stabilization of alternating structures is the result of decreasing segregation strengths. The previous study on the thermodynamically symmetric AB/BC/ABC ternary blends found that the system macrophase separates more easily when the diblocks have low segregation strengths χN, and therefore more ABC triblocks are needed to open a G^A window.[19] The shifts of stability windows for our system at different temperatures are consistent with this prediction. Moreover, the effects of segregation strengths indicate a second factor that contributes to the large differences between $\phi^*_{G^A,ISO}$ here and $\phi^*_{G^A,ABC}$ in the idealized system, in addition to the domain-size mismatch. In the previous work by Park et al.,[19] a higher χN = 20 for the diblocks was chosen, while in the IS/SO/ISO system we study, χN_{IS} is 13.1 and χN_{SO} is 17.1 at 100 °C. Correspondingly, less than 1% of ϕ_{ABC} is needed to open the G^A stability window, which is much less than $\phi^*_{G^A,ISO}$ = 6.2% according to our calculations. To stabilize G^A against macrophase separation, larger χN values for the diblocks are preferred, inferring that increasing the degree of polymerization of diblock polymers may broaden the stability window and reduce the amount of triblocks needed to stabilize G^A.

In addition to the subtle balance between macrophase separation and formation of alternating phases, temperature also affects the competition between G^A and L^A. If we only consider the building blocks formed by the diblocks, i.e., the change in equilibrium morphology of IS diblock polymer melts from DG to BCC as temperature increases, we should not expect L^A to become more stable because of the larger preferred interfacial curvatures of IS diblocks. However, wider stability windows of L^A and narrower windows of G^A are observed at higher temperatures. A possible explanation is that as temperature increases, the entropic part of the free energy becomes more important, and thus the chain stretching in the nonuniform domains of G^A becomes more problematic. A similar argument can also explain why $CSC_{6,O}$ outcompetes C_3C_6 at higher temperature. $CSC_{6,O}$ has a more uniform S domain and a continuous I domain as illustrated in Figure 6(c), which produces a higher configurational and translational entropy than the other two competing phases. As a result, the stability window of C_3C_6 is taken over by $CSC_{6,O}$ at 150 °C.

Effects of Block Volume Fractions. In the previous discussion, we demonstrated that both matching the domain sizes of DG-forming diblock polymers and lowering the temperature help enhance the stability of G^A against the competing L^A phase. An alternative method to enhance the relative stability of G^A is to tune the monomer volume fractions of the diblocks, i.e., $f_{I(IS)}$ and $f_{O(SO)}$. As in the previous discussion, the formation of G^A is relatively insensitive to the exact structure that the diblock copolymers tend to form in the neat melt, provided the monomer volume fractions of the diblocks are close to the DG-forming window. This suggests the potential to destabilize L^A by increasing the preferred interfacial curvature of the diblocks, which can be

https://doi.org/10.1021/acs.macromol.2c02485
Macromolecules 2023, 56, 2568−2577

achieved by tuning the block volume fractions to a more asymmetric regime. In Figure 8, portions of ternary phase diagrams with different $f_{I(IS)}$ demonstrate that a slight decrease in $f_{I(IS)}$ from 0.41 to 0.40 results in a much narrower L^A stability window. Further decreasing $f_{I(IS)}$ to 0.39 causes L^A to disappear. Due to the destabilization of L^A, a slightly wider G^A stability window is predicted at more asymmetric $f_{I(IS)}$, even though the IS diblocks self-assemble into C_6 phase in a neat melt.

CONCLUSIONS

In this work, we study the phase behavior of an IS/SO/ISO ternary blend at low concentrations of ISO triblock terpolymers using SCFT calculations. In the computed ternary phase diagrams, G^A stability windows are identified, indicating the feasibility of producing G^A using realistic block polymer blends. Our calculations unveil the remarkable sensitivity to molecular asymmetry in accessing network phases; unlike in the thermodynamically symmetric system, the domain-size matching between the immiscible I and O domains becomes a problem in this practical model of polymer blends. Our results show that the domain-size mismatch between I and O domains decreases the stability of G^A compared to the competing L^A phase. Thus, in the experimental design of ternary blends for self-assembled G^A, the domain sizes of the DG formed by IS and SO diblock copolymer melts should be comparable. The domain-size mismatch also leads to an unusual cylindrical packing in the cylinder-forming region of the ternary phase diagram. The destabilization of C_3C_6 and the stabilization of C_2C_6 indicate that properly designing a blend system with domain-size mismatch can potentially stabilize other non-canonical phases. For example, in a recent SCFT study by Magruder et al.,[43] a binary blend of AB and BC diblock copolymers that self-assemble into BCC phases of different domain sizes in their neat melts can produce Laves phases. In addition to the domain-size mismatch, the effects of temperature and other design parameters such as the diblock volume fraction are also explored. According to our calculations, lower temperature is preferred for the formation of G^A, because it enhances the relative stability of G^A compared to the macrophase-separated state of diblock-rich phases and the competing L^A phase. The results of varied diblock volume fractions suggest that tuning the preferred curvature of one of the blend components can alter the competition between alternating structures. All these calculations offer useful insights into the experimental design of a blend system for producing G^A.

ASSOCIATED CONTENT

Supporting Information

The Supporting Information is available free of charge at https://pubs.acs.org/doi/10.1021/acs.macromol.2c02485.

Illustration of candidate phases, additional free energy data and phase diagram results, and density profiles from SCFT solutions (PDF)

AUTHOR INFORMATION

Corresponding Author

Kevin D. Dorfman − *Department of Chemical Engineering and Materials Science, University of Minnesota−Twin Cities, Minneapolis, Minnesota 55455, United States;* orcid.org/0000-0003-0065-5157; Email: dorfman@umn.edu

Authors

Pengyu Chen − *Department of Chemical Engineering and Materials Science, University of Minnesota−Twin Cities, Minneapolis, Minnesota 55455, United States;* orcid.org/0000-0003-4545-309X

Frank S. Bates − *Department of Chemical Engineering and Materials Science, University of Minnesota−Twin Cities, Minneapolis, Minnesota 55455, United States;* orcid.org/0000-0003-3977-1278

Complete contact information is available at: https://pubs.acs.org/10.1021/acs.macromol.2c02485

Notes

The authors declare no competing financial interest.

ACKNOWLEDGMENTS

The authors thank Dr. So Jung Park for assistance with the SCFT calculations. This work was supported primarily by the National Science Foundation through the University of Minnesota MRSEC under Award Number DMR-2011401. Computational resources were provided in part by the Minnesota Supercomputing Institute (MSI).

REFERENCES

(1) Maurer, W. W.; Bates, F. S.; Lodge, T. P.; Almdal, K.; Mortensen, K.; Fredrickson, G. H. Can a single function for χ account for block copolymer and homopolymer blend phase behavior? *J. Chem. Phys.* **1998**, *108*, 2989−3000.

(2) Lequieu, J.; Quah, T.; Delaney, K. T.; Fredrickson, G. H. Complete photonic band gaps with nonfrustrated ABC bottlebrush block polymers. *ACS Macro Lett.* **2020**, *9*, 1074−1080.

(3) Li, L.; Schulte, L.; Clausen, L. D.; Hansen, K. M.; Jonsson, G. E.; Ndoni, S. Gyroid nanoporous membranes with tunable permeability. *ACS Nano* **2011**, *5*, 7754−7766.

(4) Crossland, E. J.; Kamperman, M.; Nedelcu, M.; Ducati, C.; Wiesner, U.; Smilgies, D. M.; Toombes, G. E.; Hillmyer, M. A.; Ludwigs, S.; Steiner, U.; Snaith, H. J. A bicontinuous double gyroid hybrid solar cell. *Nano Lett.* **2009**, *9*, 2807−2812.

(5) Meuler, A. J.; Hillmyer, M. A.; Bates, F. S. Ordered network mesostructures in block polymer materials. *Macromolecules* **2009**, *42*, 7221−7250.

(6) Oka, T.; Ohta, N.; Hyde, S. Polar−nonpolar interfaces of normal bicontinuous cubic phases in nonionic surfactant/water systems are parallel to the gyroid surface. *Langmuir* **2020**, *36*, 8687−8694.

(7) Chen, P.; Mahanthappa, M. K.; Dorfman, K. D. Stability of cubic single network phases in diblock copolymer melts. *J. Polym. Sci.* **2022**, *60*, 2543−2552.

(8) Michielsen, K.; Stavenga, D. G. Gyroid cuticular structures in butterfly wing scales: Biological photonic crystals. *J. R. Soc. Interface* **2008**, *5*, 85−94.

(9) Saranathan, V.; Osuji, C. O.; Mochrie, S. G.; Noh, H.; Narayanan, S.; Sandy, A.; Dufresne, E. R.; Prum, R. O. Structure, function, and self-assembly of single network gyroid ($I4_132$) photonic crystals in butterfly wing scales. *Proc. Natl. Acad. Sci. U. S. A.* **2010**, *107*, 11676−11681.

(10) Saranathan, V.; Narayanan, S.; Sandy, A.; Dufresne, E. R.; Prum, R. O. Evolution of single gyroid photonic crystals in bird feathers. *Proc. Natl. Acad. Sci. U. S. A.* **2021**, *118*, No. e2101357118.

(11) Maldovan, M.; Urbas, A. M.; Yufa, N.; Carter, W. C.; Thomas, E. L. Photonic properties of bicontinuous cubic microphases. *Phys. Rev. B* **2002**, *65*, 165123.

(12) Xie, Q.; Qiang, Y.; Li, W. Single gyroid self-assembled by linear BABAB pentablock copolymer. *ACS Macro Lett.* **2022**, *11*, 205−209.

(13) Mogi, Y.; Mori, K.; Matsushita, Y.; Noda, I. Tricontinuous morphology of triblock copolymers of the ABC type. *Macromolecules* **1992**, *25*, 5412−5415.

(14) Matsen, M. W. Gyroid versus double-diamond in ABC triblock copolymer melts. *J. Chem. Phys.* **1998**, *108*, 785−796.
(15) Epps, T. H.; Cochran, E. W.; Bailey, T. S.; Waletzko, R. S.; Hardy, C. M.; Bates, F. S. Ordered network phases in linear poly(isoprene-b-styrene-b-ethylene oxide) triblock copolymers. *Macromolecules* **2004**, *37*, 8325−8341.
(16) Tyler, C. A.; Qin, J.; Bates, F. S.; Morse, D. C. SCFT study of nonfrustrated ABC triblock copolymer melts. *Macromolecules* **2007**, *40*, 4654−4668.
(17) Vignolini, S.; Yufa, N. A.; Cunha, P. S.; Guldin, S.; Rushkin, I.; Stefik, M.; Hur, K.; Wiesner, U.; Baumberg, J. J.; Steiner, U. A 3D optical metamaterial made by self-assembly. *Adv. Mater.* **2012**, *24*, OP23−OP27.
(18) Hur, K.; Francescato, Y.; Giannini, V.; Maier, S. A.; Hennig, R. G.; Wiesner, U. Three-dimensionally isotropic negative refractive index materials from block copolymer self-assembled chiral gyroid networks. *Angew. Chem., Int. Ed.* **2011**, *50*, 11985−11989.
(19) Park, S. J.; Bates, F. S.; Dorfman, K. D. Alternating Gyroid in Block Polymer Blends. *ACS Macro Lett.* **2022**, *11*, 643−650.
(20) Yang, K. C.; Yao, C. T.; Huang, L. Y.; Tsai, J. C.; Hung, W. S.; Hsueh, H. Y.; Ho, R. M. Single gyroid-structured metallic nanoporous spheres fabricated from double gyroid-forming block copolymers via templated electroless plating. *NPG Asia Mater.* **2019**, *11*, 9.
(21) Bailey, T. S.; Hardy, C. M.; Epps, T. H.; Bates, F. S. A noncubic triply periodic network morphology in poly(isoprene-b-styrene-b-ethylene oxide) triblock copolymers. *Macromolecules* **2002**, *35*, 7007−7017.
(22) Qin, J.; Bates, F. S.; Morse, D. C. Phase behavior of nonfrustrated ABC triblock copolymers: weak and intermediate segregation. *Macromolecules* **2010**, *43*, 5128−5136.
(23) Chang, A. B.; Bates, F. S. The ABCs of block polymers. *Macromolecules* **2020**, *53*, 2765−2768.
(24) Hückstädt, H.; Göpfert, A.; Abetz, V. Influence of the block sequence on the morphological behavior of ABC triblock copolymers. *Polymer* **2000**, *41*, 9089−9094.
(25) Matsen, M. W.; Schick, M. Stable and unstable phases of a diblock copolymer melt. *Phys. Rev. Lett.* **1994**, *72*, 2660−2663.
(26) Matsen, M. W. The standard Gaussian model for block copolymer melts. *J. Phys.: Condens. Matter* **2002**, *14*, R21.
(27) Arora, A.; Qin, J.; Morse, D. C.; Delaney, K. T.; Fredrickson, G. H.; Bates, F. S.; Dorfman, K. D. Broadly accessible self-consistent field theory for block polymer materials discovery. *Macromolecules* **2016**, *49*, 4675−4690.
(28) Cheong, G. K.; Chawla, A.; Morse, D. C.; Dorfman, K. D. Open-source code for self-consistent field theory calculations of block polymer phase behavior on graphics processing units. *Eur. Phys. J. E* **2020**, *43*, 15.
(29) Rasmussen, K. Ø.; Kalosakas, G. Improved numerical algorithm for exploring block copolymer mesophases. *J. Polym. Sci. B: Polym. Phys.* **2002**, *40*, 1777−1783.
(30) Cochran, E. W.; Morse, D. C.; Bates, F. S. Design of ABC triblock copolymers near the ODT with the random phase approximation. *Macromolecules* **2003**, *36*, 782−792.
(31) Arora, A.; Pillai, N.; Bates, F. S.; Dorfman, K. D. Predicting the phase behavior of ABAC tetrablock terpolymers: Sensitivity to Flory−Huggins interaction parameters. *Polymer* **2018**, *154*, 305−314.
(32) Willis, J. D.; Beardsley, T. M.; Matsen, M. W. Simple and accurate calibration of the Flory−Huggins interaction parameter. *Macromolecules* **2020**, *53*, 9973−9982.
(33) Jeon, H. G.; Hudson, S. D.; Ishida, H.; Smith, S. D. Microphase and macrophase transitions in binary blends of diblock copolymers. *Macromolecules* **1999**, *32*, 1803−1808.
(34) Kimishima, K.; Jinnai, H.; Hashimoto, T. Control of self-assembled structures in binary mixtures of AB diblock copolymer and AC diblock copolymer by changing the interaction between B and C block chains. *Macromolecules* **1999**, *32*, 2585−2596.
(35) Frielinghaus, H.; Hermsdorf, N.; Almdal, K.; Mortensen, K.; Messé, L.; Corvazier, L.; Fairclough, J. P. A.; Ryan, A. J.; Olmsted, P. D.; Hamley, I. W. Micro− vs. macro-phase separation in binary blends of poly(styrene)-poly(isoprene) and poly(isoprene)-poly(ethylene oxide) diblock copolymers. *Europhys. Lett.* **2001**, *53*, 680−686.
(36) Brinkmann, S.; Stadler, R.; Thomas, E. L. New structural motif in hexagonally ordered cylindrical ternary (ABC) block copolymer microdomains. *Macromolecules* **1998**, *31*, 6566−6572.
(37) Wang, C.; Lee, D. H.; Hexemer, A.; Kim, M. I.; Zhao, W.; Hasegawa, H.; Ade, H.; Russell, T. P. Defining the nanostructured morphology of triblock copolymers using resonant soft X-ray scattering. *Nano Lett.* **2011**, *11*, 3906−3911.
(38) Vaidya, N. Y.; Han, C. D. Temperature−composition phase diagrams for binary blends consisting of chemically dissimilar diblock copolymers. *Macromolecules* **2000**, *33*, 3009−3018.
(39) Matsen, M. W.; Bates, F. S. Origins of complex self-assembly in block copolymers. *Macromolecules* **1996**, *29*, 7641−7644.
(40) Dong, Q.; Li, W. Effect of molecular asymmetry on the formation of asymmetric nanostructures in ABC-type block copolymers. *Macromolecules* **2021**, *54*, 203−213.
(41) Asai, Y.; Takano, A.; Matsushita, Y. Asymmetric double tetragonal domain packing from ABC triblock terpolymer blends with chain length difference. *Macromolecules* **2016**, *49*, 6940−6946.
(42) Xie, N.; Liu, M.; Deng, H.; Li, W.; Qiu, F.; Shi, A.-C. Macromolecular metallurgy of binary mesocrystals via designed multiblock terpolymers. *J. Am. Chem. Soc.* **2014**, *136*, 2974−2977.
(43) Magruder, B. R.; Park, S. J.; Collanton, R. P.; Bates, F. S.; Dorfman, K. D. Laves phase field in a diblock copolymer alloy. *Macromolecules* **2022**, *55*, 2991−2998.

https://doi.org/10.1021/acs.macromol.2c02485
Macromolecules 2023, 56, 2568−2577